ACOUSTIC PHONON SPECTRUM MODIFICATION IN THREE-LAYERED HETEROSTRUCTURES

Evghenii P. Pokatilov and Denis L. Nika
Department of Theoretical Physics
State University of Moldova
Kishinev, Republic of Moldova

and

Alexander A. Balandin
Nano-Device Laboratory
Department of Electrical Engineering
University of California - Riverside
Riverside, California 92521 U.S.A.

ABSTRACT

We theoretically investigated acoustic phonon spectrum and phonon group velocities in three-layered heterostructures with the nanoscale core layer thickness. The equations of motion for different phonon polarizations in the anisotropic medium approximation, which allowed us to include specifics of the wurtzite lattice were derived. Basing on our model we calculated phonon density of states and phonon group velocity. It has been demonstrated that the phonon group velocity in the core layer can be made higher or lower than in corresponding bulk material by a proper selection of the cladding material thickness.

1. INTRODUCTION

Acoustic phonons in bulk semiconductors are characterized by nearly linear dispersion relation near the Brillouin zone center, wide continuous spectral range and high population densities even at low temperature. In semiconductor heterostructures and nanostructures with feature size W smaller than the phonon mean free path Λ, the acoustic phonon spectrum can undergo strong modification [1]. This modification is particularly strong when the structure feature size becomes much smaller than the phonon mean free path, $W<<\Lambda$, and approaches the scale of the dominant phonon wavelength $\lambda_d \cong 1.48V_S\hbar/k_BT$ [2]. Here k_B is the Boltzmann constant, T is the absolute temperature, $\hbar$ is the Plank's constant, and V_S is the sound velocity. For many crystalline materials this scale is on the order of nanometer at room temperature.

The investigation of acoustic phonon spectra in the context of layered structures dates back to as early as half a century ago. Theoretically, the folded acoustic phonons in layered medium have been studied by Rytov [3]. Later, the folded phonons have been observed experimentally in quantum well superlattices (QWS) [4]. Many theoretical results for quantized phonons in free-standing films, nanowires and spherical quantum dots were obtained using the analogy with acoustics and classical mechanics [5-7]. Dispersion of dilatational, flexural and shear vibrational modes in thin films has been described in Ref. [5], dispersion of hybrid thickness and width modes has been obtained in Ref. [6]. More recently, phonon dispersion in quantum dot superlattices (QDS) has been calculated taking into account elastic constants of both dot and barrier material [8]. The cited above results for confined phonons in thin films and nanowires were obtained under the assumption of the free-surface, e.g. free standing, or clamped surface boundary conditions [5-7]. The important question for phonon transport in the plane of a thin film or along the axis of a nanowire, which has not been properly addressed yet, is the effect of the surrounding material (matrix, barrier, or cladding) on acoustic phonon spectra of ultra-thin films and heterostructures. In this paper we address this issue and investigate acoustic phonon spectrum of a three-layered semiconductor structure with ultra-thin inside layer and cladding (barrier) material. We carry out our calculations for wurtzite AlN/GaN/AlN heterostructures. The rest of the paper is organized as follows. In section 2 we derive the equations of motion for the elastic vibrations in the three-layered structure. Results and discussion are presented in section 3. We give our conclusions in section 4.

2. THEORETICAL MODEL

In order to investigate the role of the cladding material on acoustic phonon spectrum of ultra-thin films we consider a free-standing single thin film, e.g. slab, and a free-standing three-layered structure, e.g. double heterostructure. Both structures have a nanometer feature size along the growth direction. A schematic view of the slab and three-layered structure are shown in the insets to Fig. 1 and Fig.3, respectively. The axis X_1 and axis X_2 in the Cartesian coordinate system are in the plane of the layers while the axis X_3 is directed perpendicular to the layer surfaces. The layer thickness is denoted by d_i (i=1,2,3). As an example system we consider AlN/GaN/AlN heterostructure. GaN and related compounds crystallize in wurtzite (hexagonal) or zinc blende (cubic) lattice. Here we consider wurtzite GaN as more technologically important. It is further assumed that the layers have hexagonal symmetry with a crystallographic axis c directed along a coordinate axis X_3.

The equation of motion for elastic vibrations in an anisotropic medium can be written as

$$\rho \frac{\partial^2 U_m}{\partial t^2} = \frac{\partial \sigma_{mi}}{\partial x_i}, \quad (1)$$

where $\vec{U}(U_1, U_2, U_3)$ is the displacement vector, ρ is the mass density of the material, σ_{mi} is the elastic stress tensor given by $\sigma_{mi} = c_{mikj} U_{kj}$, and $U_{kj} = \frac{1}{2}(\frac{\partial U_k}{\partial x_j} + \frac{\partial U_j}{\partial x_k})$ is the strain tensor. When taking derivatives in Eq. (1), one has to take into account that the system is non-uniform along the X_3 axis. The elastic modules are the piece-wise functions of x_3:

$$c_{mikj} = c_{mikj}(x_3) \quad .$$

(2)

To reduce the number of subscript indexes in the coefficients c_{mikj}, we adopt the two-index notations according to the prescription:

$$1111 \to 11;\ 2222 \to 22;\ 3333 \to 33;\ 1122 \to 12;\ 1133 \to 13; 1313 \to 44; 2323 \to 55; 1212 \to 66$$

.

In crystals with hexagonal symmetry the following equalities are valid:

$$c_{1313} = c_{2323} = c_{44};\ c_{1212} = c_{66} \neq c_{44}.$$

(3)

Thus, we have six independent elastic constants to characterize the material. An application of the anisotropic continuum model allows us to explicitly include the specifics of lattice structure of wurtzite crystals. The equations of motion obtained in anisotropic medium approximation with such selection of the elastic constants will be completely different from the equations of motion in the isotropic elastic medium approximation or anisotropic medium approximation for cubic crystals. The differences start with the vibration eigenmode classification.

In our work we use classification of possible phonon polarizations on potential, solenoidal and shear [3]. The shear polarization can be distinguished from the others using the following definition

$$\rho \frac{\partial^2 U_2}{\partial t^2} = \frac{\partial \sigma_{2i}}{\partial x_i}$$

(4)

The axis X_1 is assumed to be along the propagation direction of the acoustic waves. Since the three-layered structure is homogeneous in the plane (X_1, X_2), we look for the solution of Eq. (4) in the following form

$$U_2(x_1, x_3, t) = u_2(x_3) e^{i(\omega t - kx_1)},$$

(5)

where u_2 is the amplitude of the traveling wave, ω is the phonon frequency and k is the phonon wave vector. By substituting Eq. (5) to Eq. (4) and taking into account Eqs. (2-3), one can turn the partial differential equation (4) into an ordinary second-order differential equation

$$-\rho\omega^2 u_2(x_3) = c_{44} \frac{d^2 u_2(x_3)}{dx_3^2} + \frac{dc_{44}}{dx_3} \cdot \frac{du_2(x_3)}{dx_3} - c_{66} k^2 u_2(x_3).$$

(6)

The displacement vector in the plane (X_1, X_2) can be represented by the sum of potential $\vec{u}(x_1, x_3, t)$ and solenoidal $\vec{v}(x_1, x_3, t)$ displacement vectors

$$\vec{U}(x_1, x_3, t) = \vec{u}(x_1, x_3, t) + \vec{v}(x_1, x_3, t).$$

(7)

The potential and solenoidal displacements are defined by the conditions: $curl(\vec{u}) = 0$ and $div(\vec{v}) = 0$, correspondingly. From these conditions we obtain the coupling equations for the first and third components of the vectors $\vec{u}(x_1, x_3, t)$ and $\vec{v}(x_1, x_3, t)$, which are given as

$$\frac{\partial u_3}{\partial x_1} - \frac{\partial u_1}{\partial x_3} = 0, \qquad \frac{\partial v_1}{\partial x_1} + \frac{\partial v_3}{\partial x_3} = 0$$

(8)

Using the same approach as in the case of shear waves $U_2(x_1, x_3, t)$, we look for the solutions for $u_1(x_1, x_3, t)$ and $v_3(x_1, x_3, t)$ in the following form

$$u_1(x_1, x_3, t) = u_1(x_3) e^{i(\omega t - kx_1)},\ v_3(x_1, x_3, t) = v_3(x_3) e^{i(\omega t - kx_1)}.$$

(9)

Substituting Eq. (9) in Eq. (1) and taking in consideration the coupling conditions (8), we obtain the following equations for $u_1(x_3)$ and $v_3(x_3)$:

$$-\rho\omega^2 u_1(x_3) = (c_{13} + 2c_{44})\frac{d^2u_1(x_3)}{dx_3^2} + 2\frac{dc_{44}}{dx_3}\cdot\frac{du_1(x_3)}{dx_3} - c_{11}k^2u_1(x_3),$$

(10)

$$-\rho\omega^2 v_3(x_3) = (c_{33} - c_{13} - c_{44})\frac{d^2v_3(x_3)}{dx_3^2} + (\frac{dc_{33}}{dx_3} - \frac{dc_{13}}{dx_3})\frac{dv_3(x_3)}{dx_3} - c_{44}k^2v_3(x_3)$$

(11)

From the solutions of Eqs. (10) and (11) we obtain the components u_1 and v_3. The components u_3 and v_1 are found from the coupling condition: $u_3 = -\frac{1}{ik}\frac{\partial u_1}{\partial x_3}, v_1 = \frac{1}{ik}\frac{\partial v_3}{\partial x_3}$.

The external surfaces of the three-layered structure are assumed to be free. As a result, the force components along all coordinate axes equal to zero, e.g., $P_1 = P_2 = P_3 = 0$, where $P_i = \sigma_{ik}n_k$, and $\vec{n}$ is the vector normal to the surfaces of the structure $\vec{n}$=(0,0,n_3). From here we obtain that

$$\frac{\partial U_2}{\partial x_3} = 0; \frac{\partial U_1}{\partial x_3} + \frac{\partial U_3}{\partial x_1} = 0;\ c_{13}U_{11} + c_{33}U_{33} = 0.$$

(12a) In Eq. (12a) the boundary conditions are applied to the total displacement vector $\vec{U} = \vec{u} + \vec{v}$.

According to the connections between u_3 and u_1, v_1 and v_3 we can suppose that components u_1 and v_3 are real, while components u_3 and v_1 are imaginary. Separating in equations (12a) real and imaginary parts we obtain:

$$\frac{du_1}{dx_3} = 0;\quad u_3 = 0;\quad \frac{dv_3}{dx_1} = 0;\quad v_1 = 0$$

(12b)

It is seen, that this way of separation of components U_i on imaginary and real parts gives the independent reflection of potential and solenoid waves from the structure boundaries $U_1 = u_1;\quad U_3 = v_3$.

Note, that representation of boundary conditions in this form is useful for consideration potential and solenoidal wave features due to the inhomogeneity of structure. The mixing of potential and solenoid vibrations at reflection from boundaries will be considered in another paper.

3. RESULTS AND DISCUSSION

To obtain the vibrational spectrum, e.g. phonon dispersion, of the three-layered structure we solve differential equations (6, 10-11) subject to the boundary conditions of Eq. (12b) using the finite difference method. The calculations are performed for each value of the phonon wave vector k from the interval $k \in (0, \pi/a)$, where a is the lattice constant in the plane (X_1, X_2). Since we are interested in the properties of ultra thin films (quantum wells), we assume that the structure is non-relaxed and, thus, the lattice constant is the same for both the thin film and barrier materials. The phonon dispersion is calculated for all three polarizations: potential, solenoidal, and shear. Due to the fact that the obtained results (in our case of independent potential and solenoidal polarizations) are qualitatively similar for these polarizations, in this paper we mainly discuss the potential polarization. Material parameters used in our simulations have been taken from Refs. [9-13].

In order to carry out model validation and to have reference curves for comparison with previously published results [5] we, first, calculate phonon dispersion for a slab made out of a well-known material such as GaAs. Fig. 1 shows the dispersion relation $\hbar\omega_n^p(k)$ for the potential phonon polarization in the slab of GaAs with the width d=10 nm.

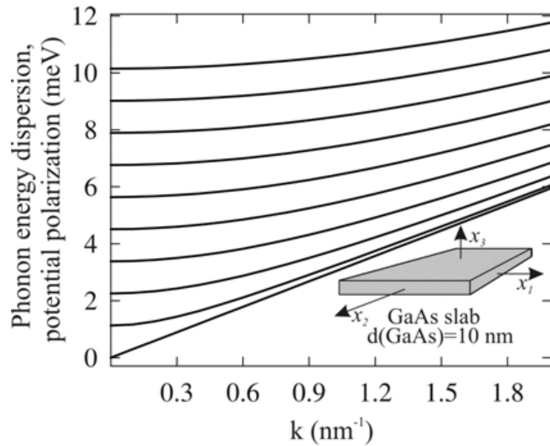

Fig. 1. Phonon energies as the functions of the phonon wave vector for the potential polarization in a 10 nm thick semiconductor slab. Results are shown for GaAs material to facilitate comparison with Refs. [5-6]. Inset shows the slab geometry and coordinate system.

One can see from this figure that (i) the phonon energy levels are equidistant at the zone center $k = 0$; (ii) the phonon branches with $n = 1, 2, \ldots$ are weakly dispersive in the vicinity of $k = 0$, and the dispersion curves can be approximated by the functional dependences of the type: $\hbar\omega_n = \hbar(\omega_{n0} + \alpha k^2)$, where $\alpha > 0$. We refer to these phonon branches as *quasi*-optical since they all have cut-off frequencies $\omega_{n0} \neq 0$.
The dispersion of these phonon branches differs from that of the optical bulk-like phonons only by the sign of α and typical values of the cut-off frequencies. The interval in k space, with the characteristic weak functional dependence of $\hbar\omega_n^{p,sl,sh}(k)$, increases with the increasing mode number n. Although not shown in the figure, there are potential, solenoidal and shear polarization bulk-like modes with the nearly linear dispersion law: $\hbar\omega_0^{p,sl,sh}(k) = v_0^{p,sl,sh}\hbar k$, where $v_0^{p,sl,sh}$ is the velocity of phonons for $n = 0$.

The characteristic features of potential polarization can be easily seen on the plots of the phonon group velocity as a function of the wave vector k, which is given as

$$v_n{}^{p,sl,sh}(k) = \frac{d}{dk}\omega_n^{p,sl,sh}(k)$$

(13)
Here the superscript denotes the polarization type, while the subscript n is used to enumerate the modes of a given polarization. We recalculate phonon dispersion for potential polarization in the slab made out of GaN material. Using the above expression we then calculate the group velocity for each mode. The group velocity for a set of potential polarization modes in GaN slab of the thickness d=6 nm is shown in Fig. 2.
The horizontal straight line in this figure indicates the phonon (sound) velocity in GaN for the longitudinal acoustic (LA) modes.

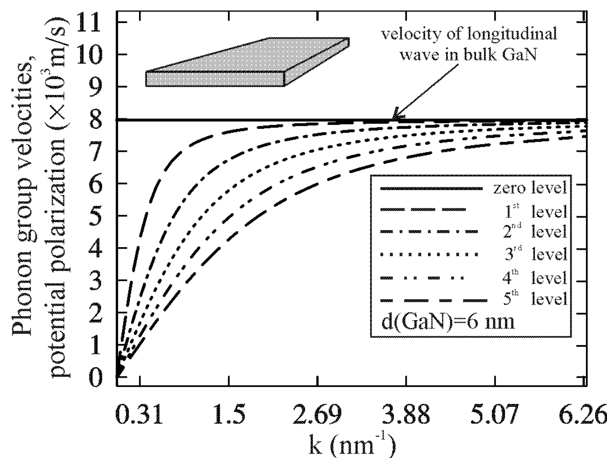

Fig.2. Phonon group velocities as the functions of the phonon wave vector for the potential polarization. Results are shown for 6.0 nm thick wurtzite GaN slab. Longitudinal sound velocity in bulk GaN is indicated with straight line.

After validating the model on the slab geometry, we have calculated phonon dispersion in the three-layered structure. Due to its practical importance, the prototype heterostructure investigated by us is AlN/GaN/AlN. Fig. 3 (a-b) shows the dispersion relation $\hbar\omega_n^p(k)$ for two three-layered AlN/GaN/AlN heterostructures.

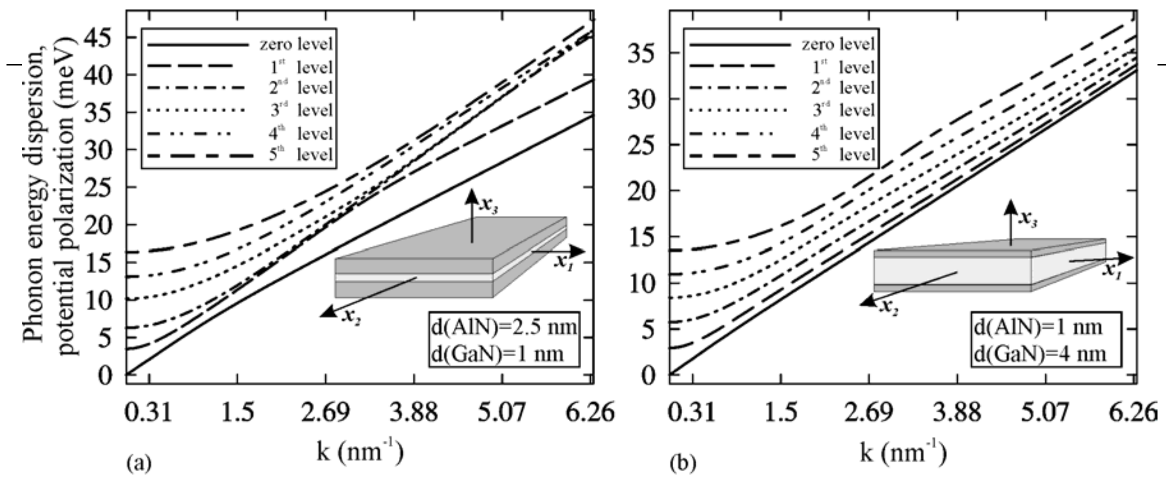

Fig. 3. Energy dispersion of the potential acoustic phonon modes in a three-layered heterostructure AlN/GaN/AlN. The results are shown for (a) the "thin core-layer" structure type I with the cladding layer thickness d_1=d_3=2.5 nm and the core layer thickness d_2=1.0 nm; as well as for (b) the "thick core-layer" structure type II with the cladding layer thickness d_1=d_3=1.0 nm and the core layer thickness d_2=4.0 nm. Inset shows the geometry of the three-layered structure.

The upper panel (Fig. 3 (a)) corresponds to the type I structure with dimensions 2.5 nm / 1 nm / 2.5 nm, while the lower panel (Fig. 3 (b)) corresponds to the type II structure with dimensions 1 nm / 4 nm /1 nm. To elucidate the effect of cladding material, we have chosen the thickness of the core layer of the type I (type II) structure to be thinner (thicker) than the cladding layer. The first observation from Fig. 3 (a-b) is that the equidistance of the phonon energy levels is slightly broken. Although as in the case of a slab the branches with modal number $n = 0$ describe the quasi bulk-like phonon modes with nearly linear dispersion relation. The influence of the cladding layers in this double heterostructure geometry on phonon spectra is manifested via more complicated behavior of the dispersion curves (compare Fig. 3 and Fig. 1).

The difference in the dispersion and the effect of the cladding are much more pronounced on the plots of the phonon group velocities. Fig. 4 (a-b) shows the phonon group velocities $v_n^p(k)$ as the function of the phonon wave vector *k*.

Fig. 4. Phonon group velocities as the functions of the phonon wave vector for the potential acoustic

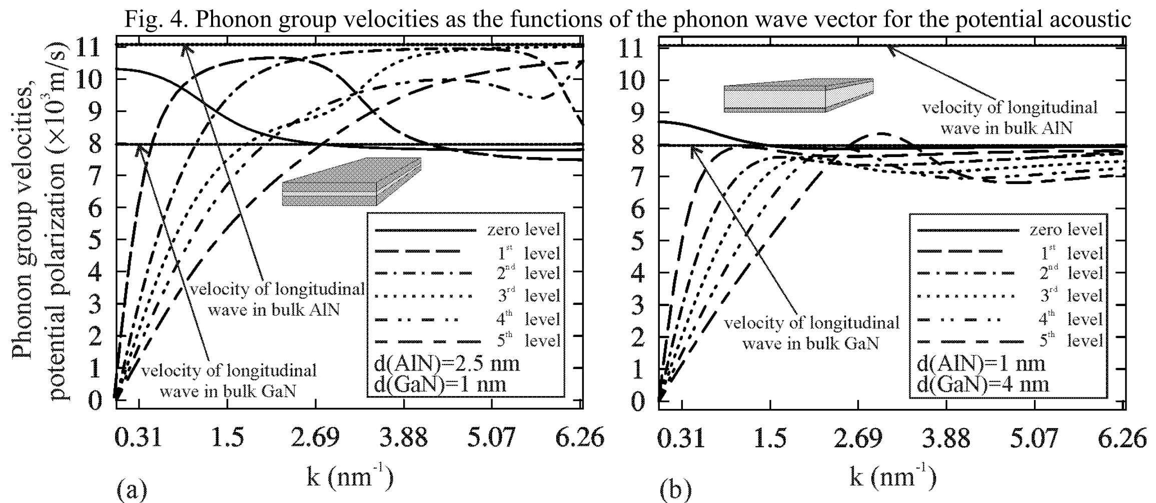

phonon modes in a three-layered heterostructure AlN/GaN/AlN. The results are shown for (a) the structure type I with the same dimensions as in the previous figure; and (b) the structure type II with the same dimensions as in the previous figure. Longitudinal sound velocities in bulk GaN and AlN are indicated with straight lines.

Unlike the velocities for the potential modes in the slab structure (see Fig. 2), the velocities $v_n^p(k)$ in these double heterostructures (three-layered structures) become non-monotonic with

maximums seen in all curves. It is interesting to note the behavior of the group velocity $v_0^p(k)$ for n=0 mode. In the thin GaN layer in both structures this velocity is larger than the group velocity v^b in bulk GaN for small values of k but it becomes smaller than the bulk GaN velocity for large values of k. The increase in the group velocity for the lowest phonon mode in the three-layered structure compared to bulk is explained by the effect of the barrier (cladding) material AlN, which has higher sound velocity compared to GaN. The increase in the group velocity is higher in Fig. 4 (a) than that in Fig. 4 (b) since in the first case the cladding material layer is thicker than the GaN core layer.

In both structures, with thin GaN layer (a) and with thick GaN layer (b), the velocities for all modes (n≠0) tend to zero for the phonon wave vector $k \to 0$, and remain smaller than the bulk velocity v^b in a wide range of k values. For small values of k, the group velocities for modes (n≠0) decrease with increasing mode number, e.g. $v_n^{p,sl}(k) > v_{n+1}^{p,sl}(k)$. But for large values of k, the functional dependence of the velocities differs strongly for specific structures. In the case of the thin-GaN-layer structure (a), the influence of the cladding AlN layers is very pronounced and the phonon velocities tend to the bulk AlN sound velocity (at large k for large n). In the case of thick-GaN-layer (b), the velocities remain smaller than the bulk GaN sound velocity for all phonon branches with $n \neq 0$ and for almost all values of k.

The behavior of the phonon dispersion $\hbar\omega_n^p(k)$ and group velocity $v_n^p(k)$ is determined by the specifics of the potential displacement vectors in the layers of the structure. As an example, in Fig. 5 (a-f) we show the components u_1 and u_3 of the displacement vector in the three-layered (type I) structure with the core GaN layer (thickness d=1 nm) embedded into AlN cladding layers of thickness d=2.5 nm each. The structure dimensions are the same as those used for Fig. 4 (a).

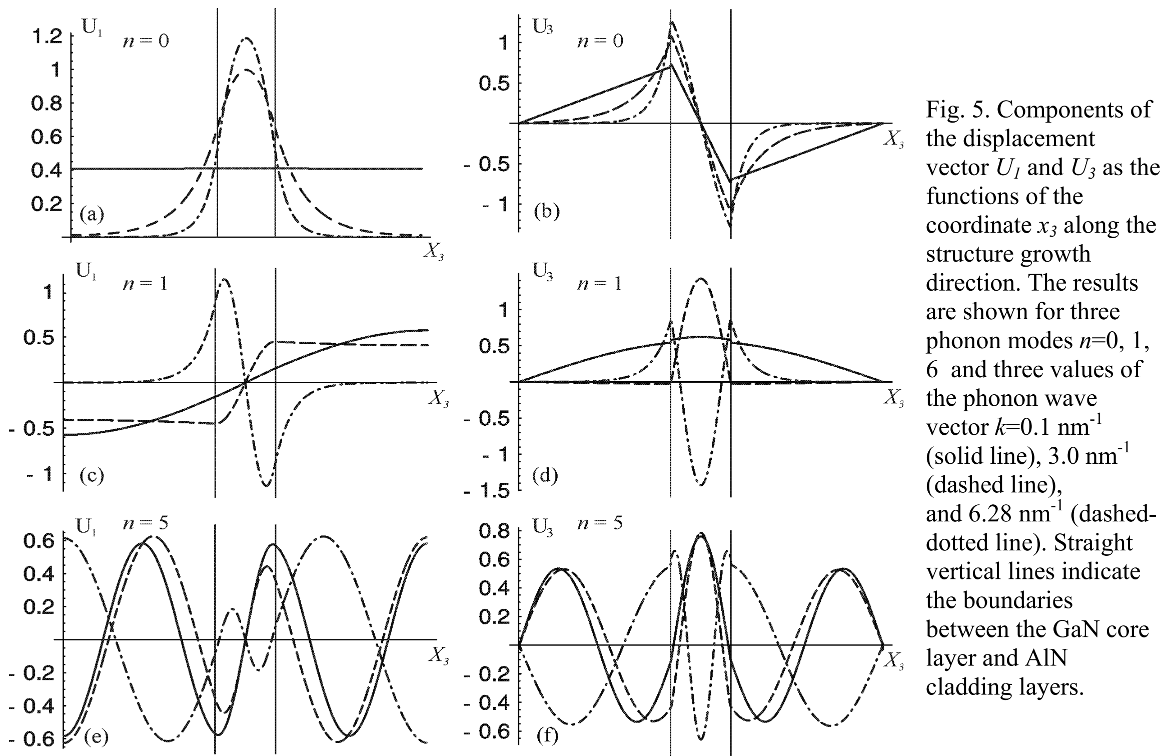

Fig. 5. Components of the displacement vector U_1 and U_3 as the functions of the coordinate x_3 along the structure growth direction. The results are shown for three phonon modes n=0, 1, 6 and three values of the phonon wave vector k=0.1 nm^{-1} (solid line), 3.0 nm^{-1} (dashed line), and 6.28 nm^{-1} (dashed-dotted line). Straight vertical lines indicate the boundaries between the GaN core layer and AlN cladding layers.

The displacements are shown for three values of the phonon wave vector: k=0.1 nm^{-1} (solid line), k=3.0 nm^{-1} (dashed line) and k=6.28 nm^{-1} (dashed-dotted line). For small values of k, the displacements of a bulk-like mode (n=0) are distributed almost uniformly among all three layers of the

structure although the total width of cladding layers is five times larger than the width of the core GaN layer. Therefore, the group velocity of this mode exceeds the sound velocity in bulk GaN (see Fig. 4 (a)). With increasing k the displacements tend to concentrate in the core layer (see Fig. 5 (a-d)) unless the mode number is too large (see Fig. 5 (e-f)). When most of the displacement is in the core layer the sound velocity decreases and becomes smaller than that in bulk GaN. In this sense this case is analogous to the decrease of the phonon group velocity in a thin slab or quantum well [1]. The effect of "slowing the phonons" in the "softer" material embedded within "harder" material is pronounced for small mode numbers n and large phonon wave vectors k. The latter is clearly seen in Fig. 5 (c, d) for the mode $n = 1$. For small and intermediate values of k the displacements extend for all structure. The displacement vectors for modes with large n are not limited to the core layers (Fig. 5 (e-f)), and correspondingly are not slowed down (see modes n=4 and n=5 in Fig. 4 (a)).

For calculation of different macroscopic characteristics of nanostructures, such as, for example, electrical and thermal conductivity, heat capacity, the knowledge of the spectral density of the phonon mode distribution, e.g. phonon density of states, is required. In the considered plane structures with very thin core layer the phonon wave vector is two-dimensional. Thus, the phonon density of states for each of the potential, solenoidal or shear polarizations with given mode number n is defined by the expression

$$f_n^{p,sl,sh}(\omega) = \frac{1}{2\pi} k_n^{p,sl,sh}(\omega) \frac{dk_n^{p,sl,sh}(\omega)}{d\omega} \quad (14)$$

The total phonon density of states for all polarizations is obtained by a summation over all n

$$F^{p,sl,sh}(\omega) = \sum_n f_n^{p,sl,sh}(\omega) \quad (15)$$

The total phonon density of states $F^{p,sl,sh}(\omega)$ for the type I three-layered structure is presented in Fig. 6.

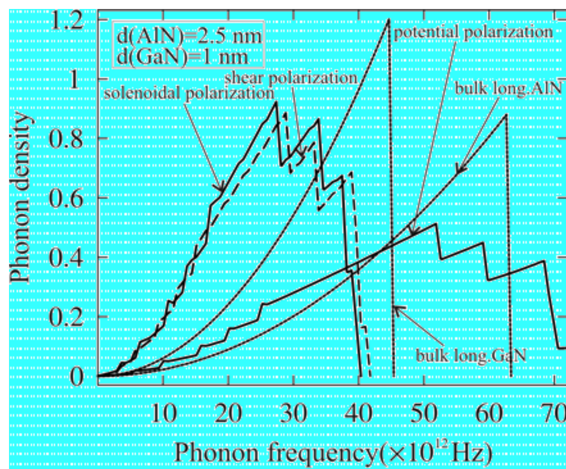

Fig. 6. Phonon density of states as the function of the phonon frequency for the potential, solenoidal and shear polarizations. The results are shown for the structure type I. Phonon density of states for longitudinal modes in bulk GaN and AlN are also shown for comparison.

For comparison, the phonon density of states for longitudinal polarizations in bulk GaN and AlN are also shown. For low phonon frequencies, the density of potential modes is lower than that of the bulk-like longitudinal modes in GaN but higher than that in bulk AlN. The oscillatory behavior of the density of states functions in the three-layered structure for each polarization is a manifestation of the phonon mode quantization and their *quasi*-optical nature (see Fig. 3). Local peaks in the density of states correspond to the onsets of new phonon branches when their cut-off frequencies are reached. Altering the phonon density of states in the three-layered structure for low frequencies can lead to the significant change in the electron-phonon scattering rates particularly for low temperatures.

The average phonon group velocity is an important characteristic that determines, for example, the lattice thermal conductivity of bulk semiconductors or nanostructures [1, 11]. We calculate the average phonon group velocity for each polarization as a velocity of a wave packet with the modes populated in accordance with the Bose-Einstein distribution function

$$\bar{v}^{p,sl,sh}(T) = \frac{\int_{\omega_{n\min}}^{\omega_{n\max}} d\omega\, n(\frac{\hbar\omega}{T}) \sum_n v_n^{p,sl,sh}(\omega) f_n^{p,sl,sh}(\omega)}{\sum_n f_n^{p,sl,sh}(\omega)}, \quad (16)$$

where $n(\frac{\hbar\omega}{T})$ is the Bose-Einstein equilibrium distribution function for phonons. Fig. 7 shows the average phonon group velocity $\bar{v}^{p,sl,sh}(T)$ as a function of temperature for the type I and type II structures.

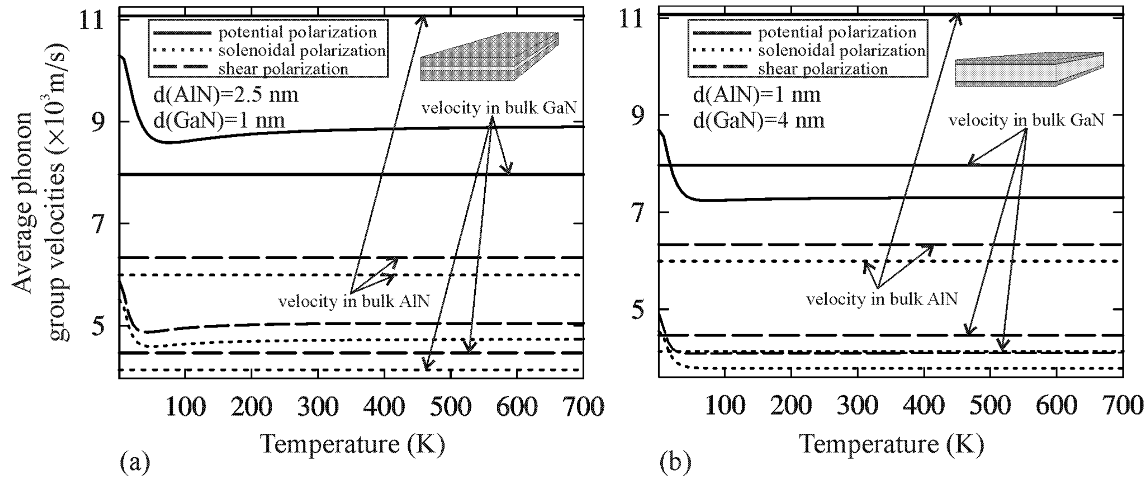

Fig. 7. Population averaged phonon group velocities as the functions of temperature for the structure type I (a); and structure type II (b). The results are shown for potential (solid line), solenoidal (dotted line), and shear (dashed line) phonon polarizations. Corresponding bulk velocities are indicated with straight lines. Note that the phonon group velocity in type I structure with very thin core layer is increased compared to bulk due to the effect of "thick" cladding layers.

The results are presented for all three phonon polarizations: potential (solid line), solenoidal (dotted line), and shear (dashed line). The corresponding velocities in bulk GaN and AlN are also shown for comparison. In the type I structure (Fig. 7 (a)), the average velocity of the thermal phonon current is considerably higher than that in the bulk GaN but lower than that in the bulk AlN. Such velocity increase is explained by the influence of the cladding layer. In the type II structure the average velocity in the core GaN layer is lower than that in the bulk GaN. The latter is due to the fact that effect of the barrier here is less pronounced and the velocity change in the core GaN layer is mostly defined by the phonon mode quantization and flattening of the polarization branches (see Figs. 3 – 4). This is in line with the prediction of the significant decrease of the phonon group velocity in a free-standing quantum well [1] and nanowire [14].

Our results demonstrate that it is possible to tune the velocity of the phonon flux in a semiconductor quantum well layer over a wide range of value. By proper selection of the material and width of the cladding layers one can either considerably increase or decrease the phonon group velocity in the core quantum well layer.

4. CONCLUSIONS

We have theoretically investigated phonon dispersion and phonon group velocity in AlN/GaN/AlN. The focus of this study was on understanding the effect of the cladding (barrier) layers on the population averaged phonon group velocity in such structures. The fact that phonon group velocity in heterostructures can be modulated bears important consequences for phonon heat transport and thermal management of electronic devices.

ACKNOWLEDGMENT

This work has been supported in part by the U.S. Civil Research and Development Foundation (CRDF).

REFERENCES

[1] A. Balandin and K.L. Wang, *Phys. Rev. B*, 58, 1544 (1998).
[2] T. Klitsner and R.O. Pohl, *Phys. Rev. B*, 36, 6551 (1987).
[3] S.M. Rytov, *Akust. Zh*. 2, 71 (1956).
[4] C.Colvard, T.A.Gant, M.V.Klein, R.Merlin, R.Fisher, H.Morkoc, A.C.Gossard, *Phys. Rev. B*, 31, 2080 (1985).
[5] N. Bannov, V. Aristov, V. Mitin and M.A. Stroscio, *Phys. Rev. B*, 51, 9930 (1995).
[6] A. Svizhenko, A. Balandin, S. Bandyopadhyay, and M.A. Stroscio, *Phys. Rev.* B, 57, 4687 (1998).
[7] M.A. Stroscio, K.W. Kim, S.G. Yu, A. Ballato, *J. Appl. Phys*., 76, 4670 (1994).
[8] O.L. Lazarenkova and A.A. Balandin, *Phys. Rev. B*, 66, 245319 (2002).
[9] O. Stier and D. Bimberg, *Phys. Rev. B*, 55, 7726 (1997).
[11] I. Vurgaftman, J.R. Meyer, L.R. Ram-Mohan, *J. Appl. Phys.*, 89, 5815 (2001)
[12] https://classes.yale.edu/eeng418a/classnotes/EE418_c13.pdf
[13] V. Bougrov, M. Levinshtein, S.L. Rumyantsev, and A. Zubrilov, *Properties of Advanced Semiconductor Materials* (J. Wiley & Sons, Inc., New York, 2001) edited by M.E. Levinshtein, S.L. Rumyantsev, M.S. Shur.
[14] J. Zou and A. Balandin, *J. Appl. Phys*., 89, 2932 (2001).